Annals Geol. Surv. Egypt. XL (2024). pp. 1-18
Manuscript id: ASGE-2309-1004

Mineralogy and Geochemistry of Hydrothermally Altered Rocks and Gold Mineralization, at Makhrag El-Ebl area, North Eastern Desert, Egypt.

BY
Ibrahim A. Salem[1], Abdelsalam M. Abo El Ela[1], Sayed Ahmed Abu Elabn[2] and Abdou M. Zeina[2]

1.Geology Department, Faculty of Science, Tanta University, Egypt.

2.Egyptian Mineral Resources Authority, Egypt.

Abstract

Makhrag El-Ebl area is located in the north Eastern Desert of Egypt. The study area is covered by Pan-African basement rocks which include granodiorites, Dokhan volcanics (dacite), syenogranites and alkali granites. Auriferous quartz veins cut through the granitic and dacitic rocks with development of alteration zones. The quartz veins display two main trends, NW-SE. and NE-SW. They vary in length from few meters to more than 100 m and in thickness from very thin veinlets to more than 20 cm. The quartz veins are massive, white and occasionally stained by iron and copper minerals. They consist mainly of quartz which carries variable amounts of gold, pyrite, native silver, hematite, goethite and barite. The altered granitic and dacitic rocks in the study area were examined using microscopic investigations, XRD, SEM-EDX analyses and whole chemical analyses of major and trace elements. The mineralogical studies accompanied by geochemical analyses for the different alteration zones revealed the existence of eight main facies include: silicification, ferrugination, chloritization, sericitization, argellic, propylitic, carbonatization and muscovite alteration.

Keywords: Hydrothermal alteration, mineralogy, petrography, geochemistry, Makhrag El-Ebl area, North Eastern Desert, Egypt

1. INTRODUCTION

Makhrag El-Ebl area is located in the north Eastern Desert of Egypt between Latitudes 27° 49' 20" - 27° 48' N and longitudes 33° 03' - 33° 05' 30" E (Fig. 1). The study area is a part of the Egyptian Nubian shield rocks which in turn a part of the Arabo-Nubian Shield (ANS).

More than 95 gold occurrences are widely distributed in the Eastern Desert of Egypt and are mostly confined to Precambrian basement rocks (El-Ramly et al, 1970). At the beginning of the Twentieth century, the majorities of the gold deposits were reopened and exploited for gold extraction by many international mining companies. Auriferous quartz veins and stockworkes of quartz veinlets cut both granodiorite and dacite rocks have been excavated for gold since ancient times. A zone of alteration usually develops along the contacts between the quartz veins and the wall rocks. The alteration may cause a change in colour, textural, mineralogical and chemical changes. The wall rock alterations are governed by i- the nature of the host rock, ii- the character of the hydrothermal solutions and iii- the temperature and pressure at which the reactions take place.

The present study deals with the detailed petrography and geochemical characteristics of the unaltered granodiorite and dacite rocks as well as the auriferous quartz veins and alteration zones. The study involves a detailed petrographic description of the hydrothermal alteration assemblages and their chemical analyses in order to elucidate the possible reactions that occurred between the original rocks and the hydrothermal fluid. The studies also determine the ore mineralogy, gold content in both quartz veins and altered rocks

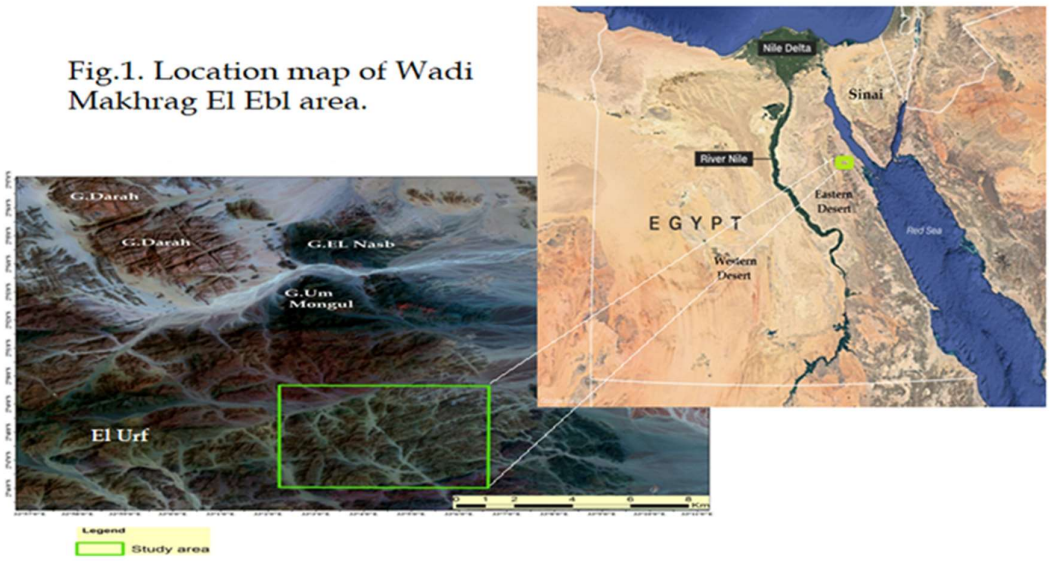

Fig.1. Location map of Wadi Makhrag El Ebl area.

2. Geologic Setting

Makhrag El-Ebl area is covered by Pan-African basement rocks. It is dominated by granodiorites,Dokhan volcanics, syenogranites, alkali granites, dykes and quartz veins. Granodiorite rocks intrude the Dokhan volcanics with clear contact. Some enclaves from Dokhan volcanic rocks occur within the granodiorite. In some places, they show boulder appearance and exfoliated due to being highly weathered

Many old working as trenches and shafts are present in the granodiorite (Fig. 2A). The Dokhan volcanics occupy the northern and north western part of the mapped area. They form moderate to high relief and dacitic in composition. The Dokhan volcanics are intruded by younger granites with sharp contact. These volcanics are sheared in NE-SW and NW-SE-directions. Hydrothermal alterations are recorded along these shear zones.

The younger granites are represented by syenogranites and alkali granites. The syenogranites occupy the southwestern and eastern parts of the mapped area. They are massive, equigranular and form moderate to high relief. The alkali granites occur as small bodies in the northern and western parts of the mapped area. They are of reddish colour, coarse grained and stained with malachite along fractures.

Auriferous quartz veins and stockworks of quartz veinlets are recorded in these rocks. Quartz veins cutting the granodiorite and alkali granite rocks (Figures, 2B and 2C). The majority of these veins are white and some of them are stained by iron and copper minerals along fractured quartz veins. These auriferous veins trend in two main directions namely NW-SE and NE-SW. These veins are ranging in length from few meters to more than l00 m. and in thickness from very thin veinlets to more than 20 cm.

3. Methodology

About 58 samples from fresh country rocks, alteration zones and quartz vein samples in Wadi Makhrag El Ebl area were petrographically examined to determine their mineral assemblages, textures and microstructures. Back-scattered imaging and energy Dispersive X-ray (EDX) analyses were carried out using Scanning Electron Microscope (SEM), Model Quanta 250 FEG at the Central Laboratories of the Egyptian Mineral Resources Authority (EMRA). SEM has accelerating voltage of 30 keV, magnification range (14x-1000000x) and resolution 1 nm. SEM was used on carefully selected spots to confirm the existence of ore and gangue minerals. Twenty country rock samples were chemically analyzed for the major oxides and trace elements. The whole-rock chemical analyses were made using Philips X-ray fluorescence (XRF) spectrometer Model PW/2404 equipped with Rh radiation tube and eight analyzing crystals. Powder pellets for trace elements and fused beads for major oxides were prepared and measured at Central Laboratories of EMRA. Eight samples from both quartz veins and the different alteration types were analyzed for gold content, using the fire assay method. X-ray diffraction analyses (XRD) of six samples were used to distinguish between the different mineral found within the different alteration zones. This technique was done at Central Laboratories of EMRA.

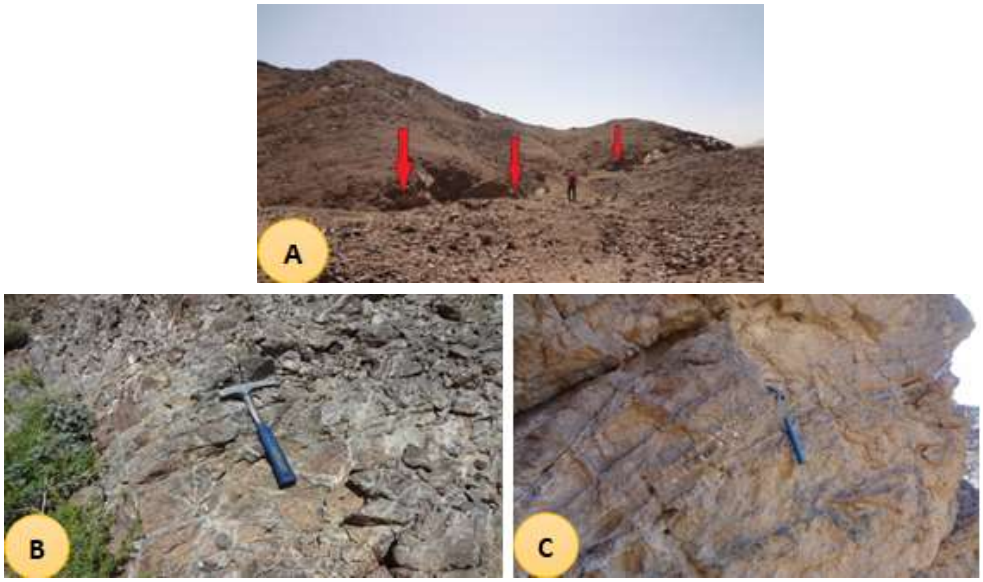

Fig.2 A: Panoramic view of old working in granodiorites. B: Field photograph showing network of quartz veinlets cutting across granodiorite. C: Field photograph showing quartz veinlets cutting across alkali granites.

a. Petrography of the country rocks

Granodiorites are massive, medium to coarse grained of grey to pinkish grey colour. Microscopically, granodiorites (Fig. 3A) showing equigranular, hypidiomorphic, perthitic, graphic and poikilitic textures. They are composed mainly of plagioclase, microcline, quartz associated with minor biotite and hornblende. Iron oxides and sphene are the main accessory minerals. Secondary minerals are represented by sericite (Fig. 3B) carbonates, chlorite and epidote.

Dacite rocks are fine to medium grained, unequigranular displaying amygdaloidal and porphyritic textures. Microscopically dacites (Fig. 3C) are composed mainly of phenocrysts of plagioclase and quartz embedded in groundmass composed of fine-grained aggregates of plagioclase, quartz, alkali feldspar, biotite and muscovite. Secondary minerals are represented

by carbonates, sericite and iron oxides. Some voidal amygdales filled by calcite, chlorite and epidote (Fig. 3D).

Syenogranites are coarse grained of light pink to Pink colour. Microscopically, syenogranites (Fig. 3E) are equigranular hypidiomorphic texture and composed essentially of quartz, alkali feldspar (perthite) (Fig. 3F), plagioclase and biotite. Secondary minerals are represented by chlorite, sericite and carbonates. Iron oxides, apatite and sphene are the accessory minerals.

Alkali granites are medium to coarse grained of red colour. They showing equigranular hypidiomorphic and myrmekitic textures (Fig. 3G). They are composed essentially of quartz, alkali feldspar (orthoclase), plagioclase, hornblende (Fig. 3H) and biotite. The accessories are zircon, sphene and apatite. Secondary minerals are chlorite, carbonate, sericite and epidote.

b. Geochemistry of the Host rocks

The geochemical studies were carried out on twenty samples (5 from granodiorites (older granites), 5 from dacites and 10 from younger granites). The results of major oxide, trace elements as well as CIPW norm are given in tables (1 and 2). P

Plotting the samples on (Na_2O +K_2O) - Si_2O diagram of (Cox et. al. 1979) show that the older granites plotted within the granodiorite field, whereas the younger granites plotted in the alkali granite and syenogranite (Fig. 4). On the normative composition Ab - Or - An ternary diagram of Streckeisen (1976), the studied older granites fall in the granodiorite field, while the younger granites plotted within the syenogranite and alkali granite fields (Fig. 5).

The magma type from which the older and younger granites were originated can be recognized using the following geochemical variation diagram.

On the ANK versus ACNK (Maniar and Piccoli, 1989), the studied older and younger granites plot in the peraluminous field (Fig.6). On the alkalinity ratio diagram (Wright 1969), the studied granodiorites, plot within the calc-alkaline field, whereas the syenogranites and alkaligranites plot within the alkaline field (Fig.7).

The tectonic setting of the studied older and younger granites can be interpreted using Pearce et al (1984) diagram (Fig.8), the studied older granites plot in the field of volcanic arc granites (VAG), but the younger granites plot in the fields of within plate.

The depth, at which the studied granitoid magmatism was crystallized at depth > 30 km (Fig.9), can be obtained by plotting the studied samples on the Rb- Sr binary diagram after Condi, 1973.

The water vapour pressure and temperature at which the studied granites were generated are estimated as given by (Tuttle and Bowen 1958) and (Luth et al, 1964). It is clear that the studied granites fall in relatively from 1 to 10 k-bar and temperature ranging from 700 to 800°C, indicating that they were probably formed at moderate levels (Figures.10 and 11).

The geochemical studies of Dokhan volcanic (dacite) in the study area were carried out on five representative samples. The rocks were chemically analyzed for their major oxides and trace elements as shown in Table 3. The studied volcanics are plotted on SiO_2 vs. Na_2O +K_2O diagrams (Fig.12) of Cox et al, 1979. Where the petrographic name was confirmed, which is dacite. On the basis of the alkalis vs. SiO_2 (Fig.13) of Irvine and Baragar, (1971), all samples are subalkaline.

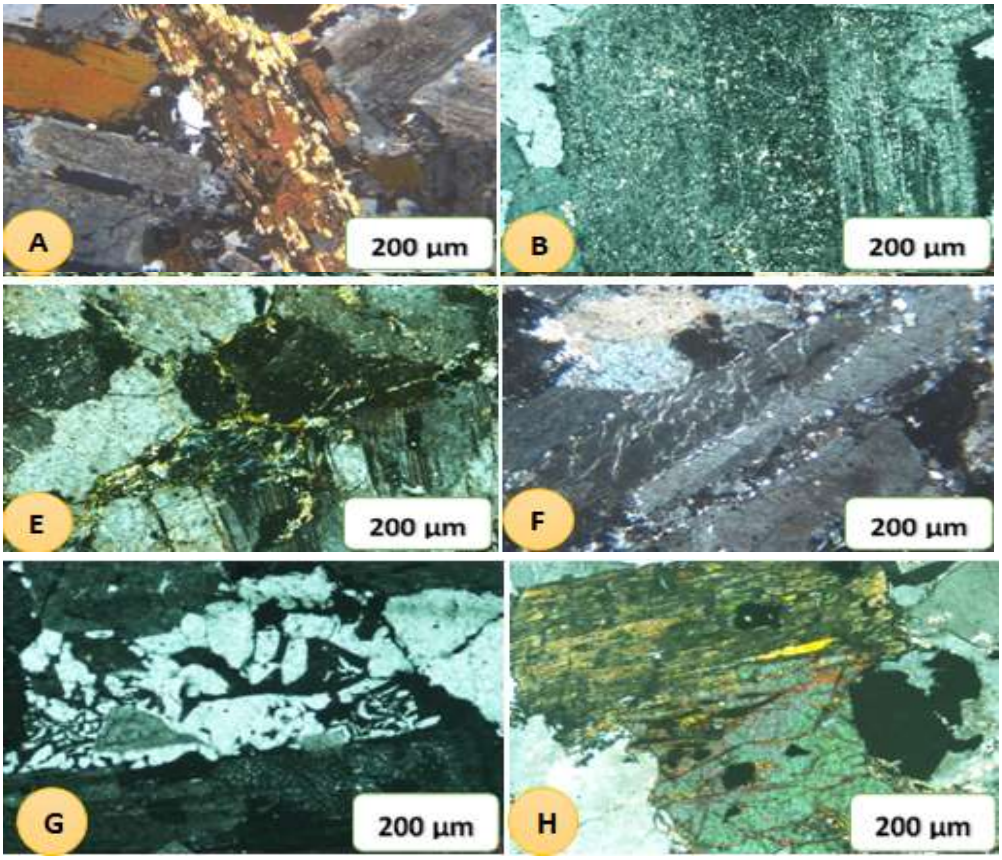

Fig.3. A: Photomicrograph of granodiorite showing flakes of biotite and altered plagioclase. (C.N). B: Photomicrograph of granodiorite showing highly altered plagioclase crystal to sericite (C.N). C: Photomicrograph of dacite showing phenocryst of plagioclase and some amygdales filled with carbonates (C.N.). D: Photomicrograph of dacite showing some rounded and irregular shape of volcanic lithic fragment embedded in fine ground mass (C.N). E: Photomicrograph of syenogranite showing biotite is highly to completely altered to chlorite and iron oxides. (C.N.) F: Photomicrograph of syenogranite showing large euhedral crystals of perthite alkali feldspar (C.N). G: Photomicrograph of alkali granite showing quartz vermicules associating plagioclase giving the myrmekitic texture. (C.N.). H: Photomicrograph of alkali granite showing alteration of hornblende to chlorite and iron oxide (C.N).

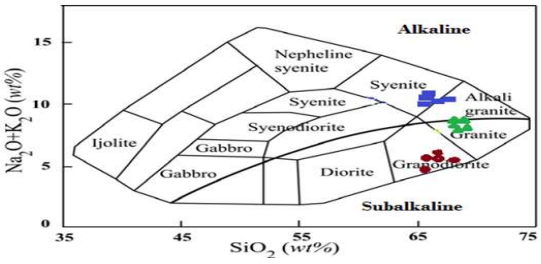

Fig.4.Total alkali versus SiO2 Diagram for the studied older granites, younger granites rocks of (Cox et al.1979) adapted by Wilson (1989) for plutonic rocks.

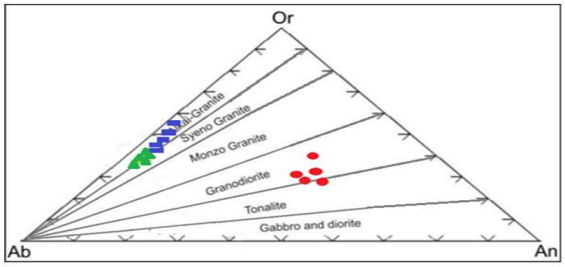

Fig.5.Ab-Or-An normative diagram (Streckeisen, 1979) of the studied granitic rocks.

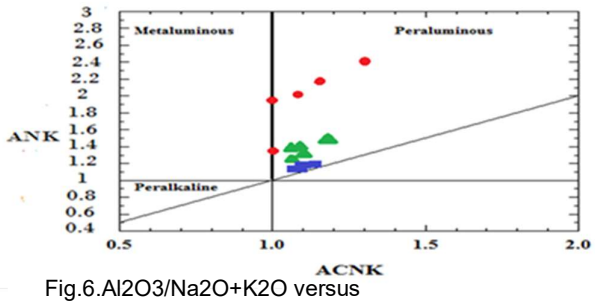

Fig.6.Al2O3/Na2O+K2O versus Al2O3/CaO+Na2O+K2O diagram (Maniar and Piccoli. 1989) of the studied granitic rocks.

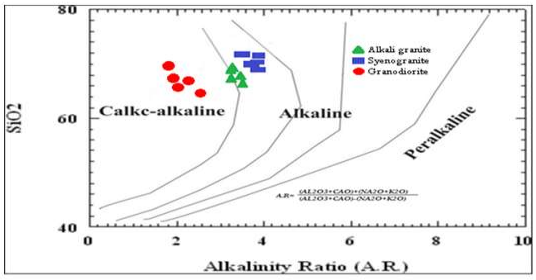

Fig.7.Alkalinity ratio (A.R)-SiO2 diagram (Wright, 1969) of the studied granitic rocks.

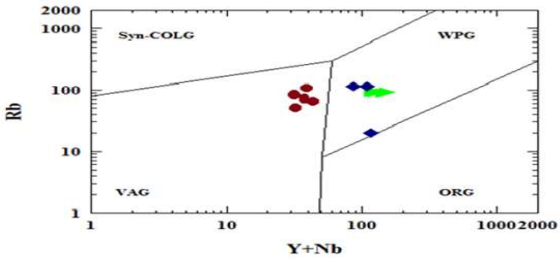

Fig.8.Y-Nb diagram (Pearce et al. 1984) of the studied of granitic rocks.

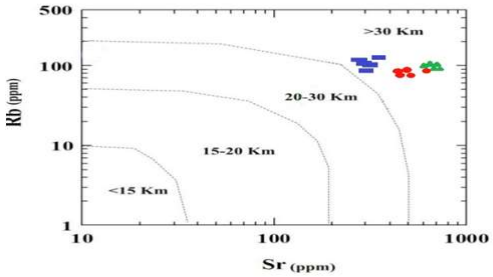

Fig.9.Rb-Sr variation diagram according to Condie (1973) for the studied granitic rocks.

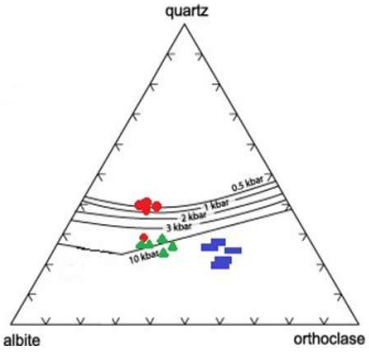

Fig.10.Q-Ab-Or ternary diagram of Tuttle and Bowen (1958) for the studied granitic rocks.

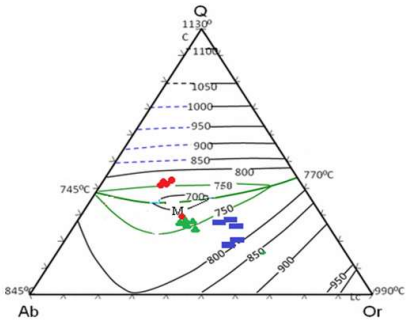

Fig.11.Q-Ab-Or ternary diagram of Tuttle and Bowen (1958) for the studied granitic rocks.

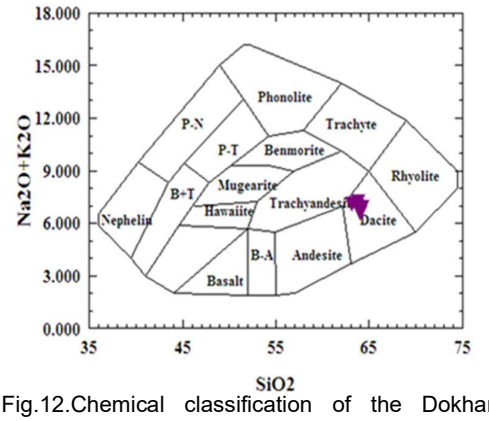

Fig.12.Chemical classification of the Dokhan Volcanics using the total alkalis versus silica (TAS) diagram of Cox et al. (1979).

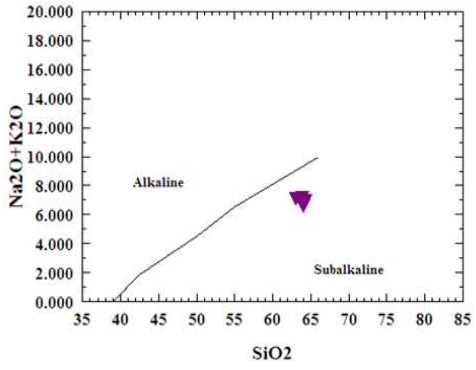

Fig.13. (TAS)Variation diagram of Irvine and Baragar (1971).

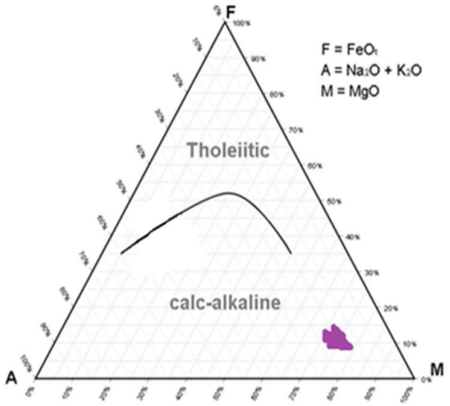

Fig.14. AFM diagram after (Irvine and Baragar, 1971)

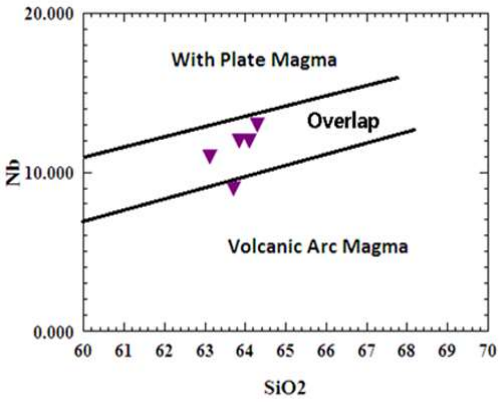

Fig.15. SiO2 versus Nb diagram (Pearce and Gale, 1977)

Fig. 16. Nb – Y tectonic discrimination diagram for the studied Dokhan volcanic, Syn-collision (Syn-COLG), volcanic arc granites (VAG), within plate granites (WPG) and ocean ridge granites (ORG), after Pearce et al. (1984).

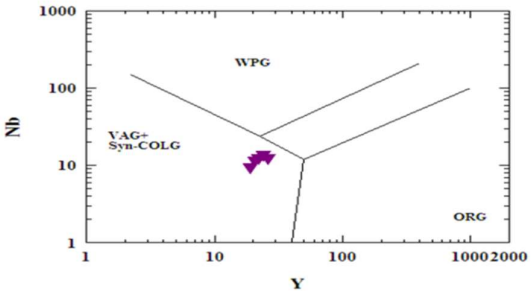

On the AFM diagram (Fig.14) of Irvine and Baragar, (1971), the dacites fall within the calc-alkaline field. On the SiO_2 vs. Nb (Fig.15) of Pearce and Gale (1977), the dacite samples fall in the overlap zone between the volcanic arc and within plate. On the Y vs. Nb diagram (Fig.16) of Pearce et al (1984), the samples fall in the volcanic arc granite.

Table 1: Chemical analysis of major oxides (wt. %), CIPW norm as well as trace elements (ppm) for the studied granodiorite rocks.

Older granites						
Rock type	Granodiorites					
S. No.	1	2	3	4	5	
Major Oxides (%)						average
SiO_2	65.86	67.02	66.58	67.80	67.65	66.98
TiO_2	0.56	0.20	0.86	0.61	0.70	0.59
Al_2O_3	14.02	16.50	15.60	14.98	14.65	15.15
FeO	3.55	2.53	2.37	2.15	2.17	2.55
Fe_2O_3	3.95	2.81	2.64	2.39	2.41	2.84
MnO	0.06	0.10	0.07	0.06	0.08	0.07
MgO	1.98	1.86	1.92	2.21	2.14	2.02
CaO	2.54	3.21	4.01	3.56	3.86	3.44
Na_2O	3.56	3.04	3.11	3.32	3.45	3.30
K_2O	3.36	2.10	2.14	2.13	2.04	2.35
P_2O_5	0.15	0.18	0.29	0.17	0.14	0.19
LOI	0.51	0.62	0.49	0.61	0.64	0.57
Total	100.10	100.17	100.08	99.99	99.93	100.05
CIPW Normative values						average
Qz	23.375	31.864	29.662	29.817	28.643	28.67
Or	22.868	14.862	15.024	14.928	14.334	16.40
Ab	31.914	27.378	27.831	29.646	30.765	29.51
Di	0.0509	0	0	0	0.3513	0.08
An	11.801	15.037	18.232	16.58	17.843	15.90
Mt	3.0571	2.1848	2.0397	1.8425	1.8554	2.20
Hy	5.9694	5.5687	4.746	5.4968	5.111	5.38
Ilm	0.6215	0.223	0.9528	0.6744	0.7728	0.65
Ap	0.3015	0.3634	0.5818	0.3403	0.2799	0.37
Trace elements (ppm)						average
Cr	133.5	62	59	57	53	72.90
Ni	50.7	11	23	17	14	23.14
Cu	1637.1	1456.5	1602.4	1564.6	1496	1551.32
Th	23.4	24.1	23.5	23.9	24.4	23.86
Ta	2.9	3.1	2.88	2.94	3.02	2.97
Zn	26	45	39	52	37	39.80
Zr	234.4	235.6	237.6	233.7	230.4	234.34
Rb	90.9	89	82	79	90	86.18
Y	15.9	13	12.5	12.7	11.9	13.20
Ba	1499.9	1504.3	1503	1522	1507	1507.24
Pb	18.5	19.3	18.7	19.3	18.9	18.94
Sr	623.8	465	485	423	462	491.76
Co	26.4	23.7	27.3	25.6	25.9	25.78
V	74.5	36	38	37	39	44.90
Nb	12.1	13.4	13.01	12.9	12.35	12.75

Table 2: Chemical analysis of major oxides (wt. %), CIPW norm as well as trace elements (ppm) for the studied alkali granites and syenogranites.

Younger granites						
Rock type	Alkali Granites					
S. No.	1	2	3	4	5	
Major Oxides (%)						average
SiO_2	67.93	67.62	68.20	67.21	68.12	67.82
TiO_2	0.61	0.54	0.50	0.56	0.52	0.55
Al_2O_3	13.31	13.54	13.43	13.44	12.91	13.33
FeO	3.16	3.55	3.22	3.43	3.39	3.35
Fe_2O_3	3.51	3.95	3.58	3.81	3.77	3.72
MnO	0.07	0.02	0.07	0.04	0.08	0.06
MgO	1.73	1.49	1.65	1.68	1.63	1.64
CaO	1.01	0.89	0.98	1.02	1.14	1.01
Na_2O	3.84	3.78	3.80	3.81	3.76	3.80
K_2O	3.95	4.08	3.87	4.25	4.02	4.03
P_2O_5	0.18	0.16	0.15	0.17	0.16	0.16
LOI	0.62	0.48	0.66	0.56	0.51	0.57
Total	99.92	100.10	100.11	99.98	100.01	100.02
CIPW Normative values						average
Qz	25.257	25.135	25.969	23.332	25.181	24.97
Or	26.997	27.907	26.618	28.983	27.458	27.59
Ab	34.112	33.578	33.722	33.836	33.32	33.71
An	4.0272	3.5622	4.0704	4.1413	4.7924	4.12
Hy	5.1306	4.879	5.1182	5.215	5.1669	5.10
Ilm	0.6739	0.5966	0.5519	0.6185	0.5731	0.60
Ap	0.3601	0.3201	0.2998	0.34	0.3193	0.33
Trace elements (ppm)						average
Cr	66	60	62	69	71	65.6
Ni	24	21	23	27	26	24.2
Cu	1702	1689	1678	1635	1789	1698.6
Th	23.4	22.8	22.6	21.7	23.5	22.8
Ta	2.69	2.61	2.45	2.48	2.96	2.638
Zn	51	49	46	45	48	47.8
Zr	310	285	296	306	301	299.6
Rb	103	100	104	99.5	100.2	101.34
Y	114	98	126	118	122	115.6
Ba	2102	2132	2203	2186	2174	2159.4
Pb	19	18	17	21	18	18.6
Sr	614	611	624	632	628	621.8
Co	23	22	21	22	24	22.4
V	70	66	69	71	74	70
Nb	32	29	28	31	30	30

Younger granites						
Rock type	Syenogranites					
S.No	1	2	3	4	5	
Major Oxides (%)						average
SiO_2	66.08	66.47	67.16	68.38	68.24	67.27
TiO_2	0.76	0.74	0.81	0.75	0.82	0.78
Al_2O_3	11.29	11.02	10.22	10.18	10.30	10.60
FeO	4.26	4.14	4.10	3.80	3.69	4.00
Fe_2O_3	4.74	4.61	4.56	4.23	4.11	4.45
MnO	0.06	0.07	0.05	0.05	0.03	0.05
MgO	1.07	1.06	1.09	1.05	1.04	1.06
CaO	0.64	0.67	0.68	0.68	0.69	0.67
Na_2O	4.93	4.84	4.78	4.69	4.86	4.82
K_2O	5.70	5.64	5.96	5.74	5.80	5.77
P_2O_5	0.24	0.27	0.30	0.26	0.27	0.27
LOI	0.47	0.51	0.46	0.65	0.47	0.51
Total	100.24	100.04	100.17	100.46	100.32	100.25
CIPW Normative values						average
Qz	14.525	16.614	19.797	22.09	21.458	18.90
Or	39.378	36.686	38.614	36.985	37.283	37.79
Ab	25.802	27.189	20.765	21.573	21.986	23.46
Hy	6.4696	6.4534	4.0955	5.8847	5.6016	5.70
Ilm	0.8507	0.5508	0.3938	0.8705	0.913	0.82
Ap	0.4865	0.5397	0.5994	0.5861	0.5444	0.55
Trace elements (ppm)						average
Cr	73.1	72.9	71.3	77	72	73.26
Ni	14.1	13.5	13.68	13.44	12.9	13.52
Cu	135.8	136.9	136.07	135.6	136.2	136.11
Th	13	12.9	13.07	12.76	12.8	12.91
Ta	2.3	2.4	2.34	2.12	2.19	2.27
Zn	16.1	15.9	15.8	16.14	16.02	15.99
Zr	200.9	200.1	199.5	199.8	200.4	200.14
Rb	115.5	116.3	114.8	116.2	115.9	115.74
Y	65	75	81	77	73	74.20
Ba	2906.2	3002.8	2986.4	2985.7	3010.4	2,978.30
Pb	14.4	14.06	14.34	14.02	14.38	14.24
Sr	309.7	314.5	311.3	322.7	318.1	315.26
Co	30.2	31.4	30.7	30.88	31.09	30.85
V	78.7	79.3	78.01	77.9	78.2	78.42
Nb	22	42	29	37	33	32.60

1. Hydrothermal alteration

The alteration zones in Wadi Makhrag El-Ebl area were mapped (Fig.17). The most prominent features indicating alteration in nature is a colour change, textures, mineralogy and chemical changes. The observed types of alteration can be formed as a result of hydrothermal solution attack on the granitic and dacitic rocks. Close to the faults, fractures and shear zones, the altered rocks are highly deformed.

In the present study, the petrographic studies accompanied by geochemical analysis (Table 3) for the different alteration zones revealed the existence of eight alteration types includes, silicification, ferrugination, chloritization, sericitization, argellic, propylitic, carbonatization and muscovite alteration.

The degree of sericitization index according to SI (Fig. 18) can be estimated by a plot of K_2O+Na_2O against K_2O /K_2O+Na_2O (Myers and Maclean, 1983). It shows that all sample fall in the hydrothermal alterations.

Silicification is an intensive alteration process affecting the dacitic and granitic host rocks. Quartz is the common minerals associated with minor amounts of alkali feldspar, plagioclase and opaque minerals (Fig. 19A). Porphyroclast texture is observed where porphyroclast of quartz imbedded in fine crystals of quartz and iron oxides (Fig. 19B). Silicification is enriched in SiO_2 (av. 96.24%) and depleted in Ti, Al, Fe, Mn, Mg, Co, Na, k and P. These minerals have been confirmed with their relative abundance by XRD technique as following: quartz (100 %) (Fig.27A).

Ferrugination zone is manifested by a network of iron oxide veinlets of brownish red colouration (Fig. 20A). Microscopically, the altered ferruginated is composed mainly of quartz, altered plagioclase associated with clay and chlorite minerals. These minerals are coasted by iron oxides (Fig. 20B). The ferruginated rocks exhibit enrichment in FeO (14.3%) and Fe_2O_3 (27.5 %.). The iron minerals are represented by hematite and goethite. The X-Ray diffraction (XRD) confirmed the presence of previously described minerals with relative of semi-quantitative estimation quartz, chlorite, hematite and kaolinite (Fig. 27B).

Argillic alterations are wide spread along the fractures in both granodiorite and dacite rocks (Figures. 21A and 21B). Mineralogically, the alkali feldspars are partially altered to Kaolinite and biotite is completely altered to chlorite with expelling of iron oxides. XRD analysis indicates that the dominant clay mineral is kaolinite and accompanied by chlorite (Fig. 27C). The argilic altered rocks show some Al_2O_3 enrichment (36.1%), FeO (2.14%), Fe_2O_3 (6. 11%), MgO (4.11%), CaO (4.9%), Na_2O (7.12%) and K_2O (5.6%), while SiO_2 (29.36%) is depleted.

Propylitic alteration is characterized by the development of secondary green minerals such as chlorite and epidote (Figures. 22A and 22B). It is commonly associated with quartz, albite plagioclase, kaolinite, calcite and muscovite, as indicated from XRD analysis (Fig. 27D). The propylitic altered rocks are enriched in SiO_2 (50.11%), Al_2O_3 (13.3 %), FeO (3.1%), $Fe2O_3$ (5.5%), Na_2O (2.95%) and K_2O and L.O.I (15.85%), but depleted MgO (0.954%) and Cao (0.82%).

Carbonatization is determined by the development of calcite (Figures. 23A and 23B). It is concentrated along joints and fissures planes. The formation of calcite can be produced by the reaction of the oxidizing meteoric waters containing abundant dissolved Co_2 with Cao was leached from the granodiorites by hydrothermal solutions. The carbonatization altered rocks are enriched in SiO_2 (av.57.71%), CaO (av.11.42 %.), Al_2O_3 (av. 8.6%), K_20 (av. 3.5%), Na_2O (av. 3.2%), FeO, (av. 2.8%) and Fe_2O_3 (av.4.57%). XRD analyses indicate that the carbonate mineral is calcite and accompanied by chlorite and kaolinite (Fig. 27E).

Sericitization is spread over a wide area with granodiorites, dacites, syenogranites and alkali granites. Sericite is most abundant with all kinds of rocks (Figures. 24A and 24B) with some quartz, chlorite and epidote. Sericite occurs as a secondary alteration product of plagioclase (Que and Allen, 1996).

Muscovite alteration is characterized by secondary muscovite with minor amounts of quartz, anorthite plagioclase and Kaolinite (Figures. 25A and 25B). The presence of these minerals have been confirmed with their relative abundance by XRD: muscovite (83%), quartz (10%), anorthite (5 %.) and Kaolinite (2 %.) (Fig. 27F). The muscovite alteration is enriched in SiO_2 (55.64 %.), Al_2O_3 (20.34%), K_2O (12.64 %.) and Na_2O (3.61%) but depleted in MgO, CaO and L.O.I.

Chloritization as replacements of mafic minerals. Chlorites mostly formed after hornblende and biotite. Chloritization consist of chlorite, biotite, epidote and sericite. Epidote and clay minerals as accessory minerals (Fig. 26A). The micas are commonly bent or kinked and feldspar is highly altered to sericite, biotite altered to chlorite, epidote as accessory minerals (Fig. 26B). The chloritization rocks exhibit enrichment in SiO_2 (51.3%), Al_2O_3 (10.8%), MgO (9.12%), FeO (7.4%), Fe_2O_3 (10.6%), while slight depletion in CaO (1.64%), Na_2O (2.94%) and K_2O (3.12%).

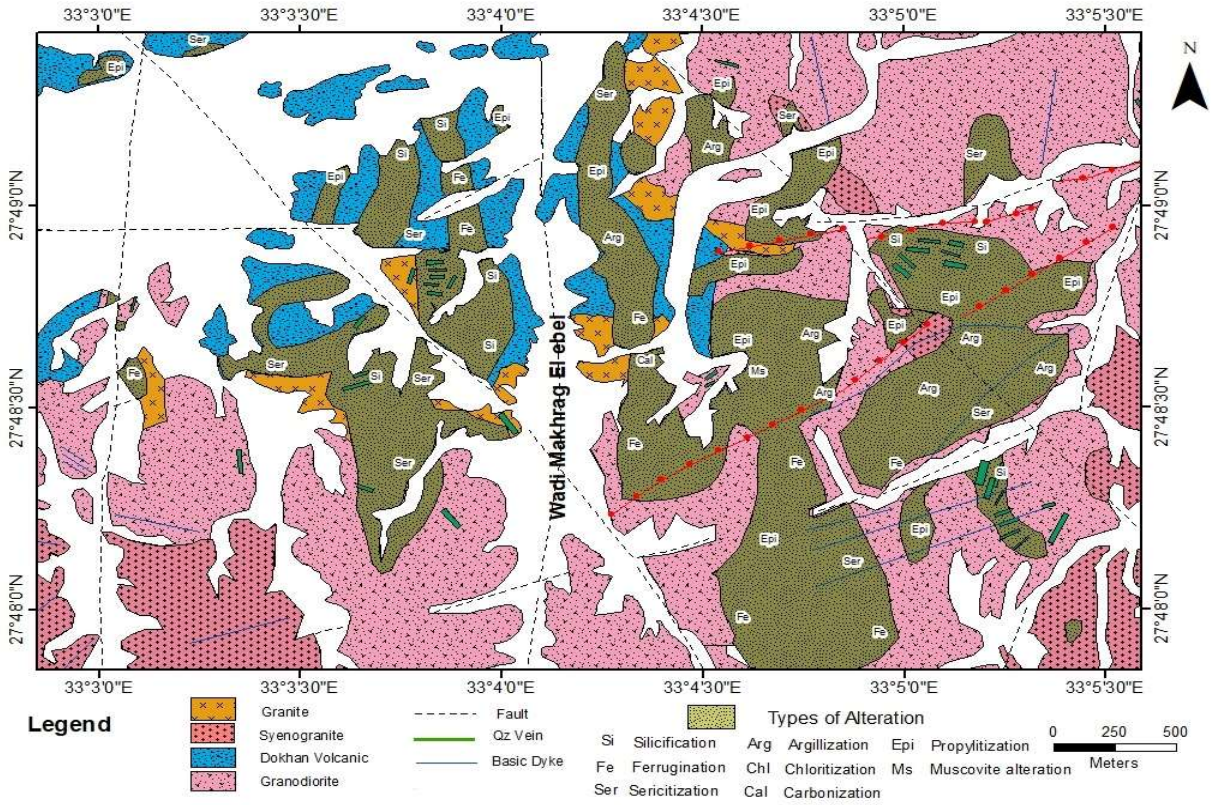

Fig.17. Geologic map showing the distribution of the alteration zones around Wadi Makhrag El Ebl area (modified after Botros and Wateit, 1997).

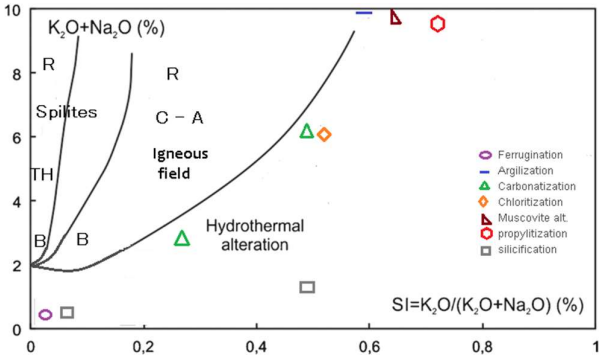

Fig.18. /K_2O+Na_2O sericitization index (SI) diagram after (Myers and Maclean, 1983). igneous fields are for calc-alkaline (C – A) and tholeiitic (TH) rocks. B=basalt. R= rhyolite.

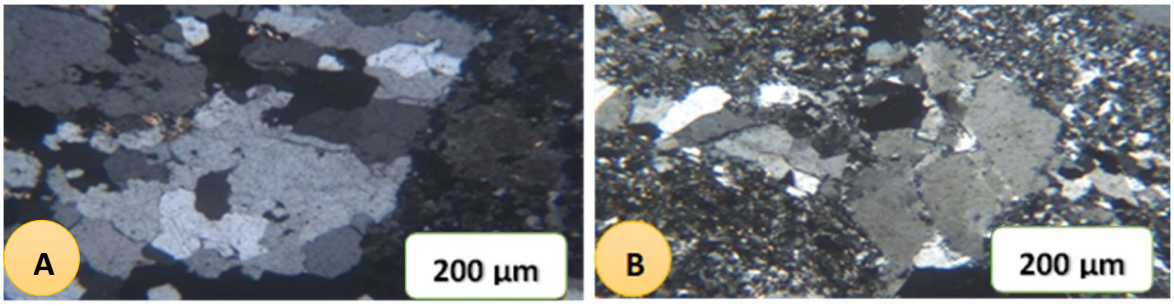

Fig. 19. A) Photomicrograph showing quartz as a major constituent associated with minor alkali-feldspar, plagioclase and iron oxides with sericite, epidote and clay minerals (C.N). B) Photomicrograph of silicification showing Porphyroclast of quartz embedded in fine crystals of quartz (C.N)..

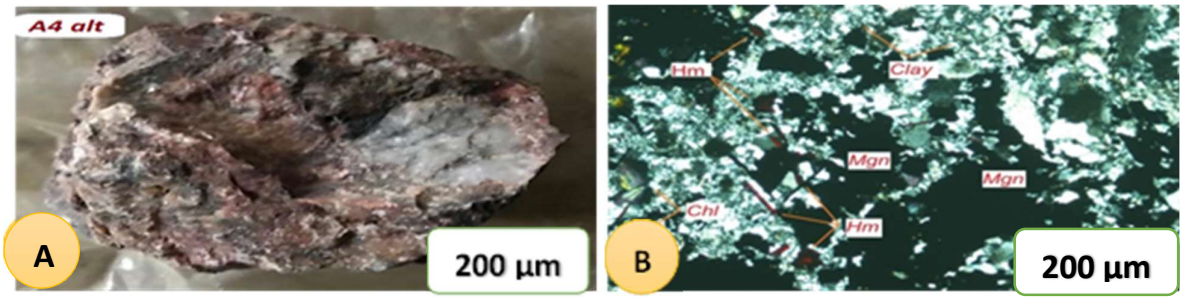

Fig. 20. A) Hand-specimen of the studied ferrugination showing reddish alteration with veinlets of quartz. B): Photomicrograph showing clay minerals are coated with iron oxides plate and alteration biotite to chlorite. (C.N). (Hm=hematite, Chl =chlorite, Mgn=magnetite, and clay = clay minerals).

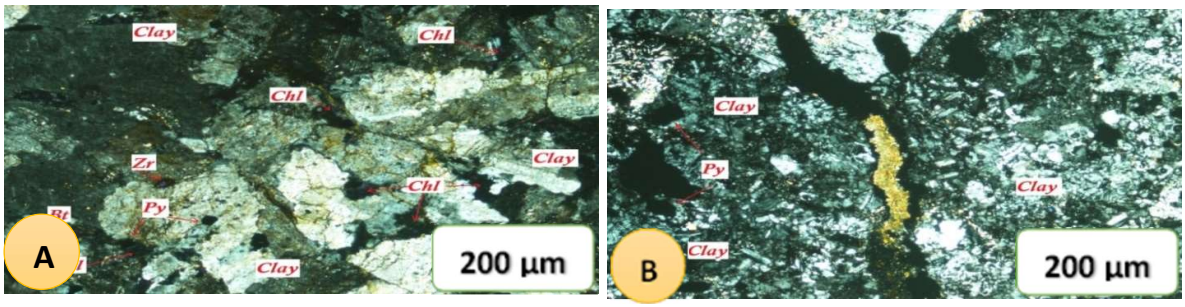

Fig. 21. A) Alkali feldspar partially to highly altered to clay minerals, biotite is highly altered to chlorite with liberation of iron oxides and pyrite crystal in altered granodiorites (C.N). B) Clay minerals, pyrite, several microveinlets filled by secondary minerals in altered dacite rocks (C.N). (Chl =chlorite, Ms= muscovite, Bt= biotite, clay = clay minerals, Ser= sericite Pla=plagioclase, Py= pyrite and Zr= zircon).

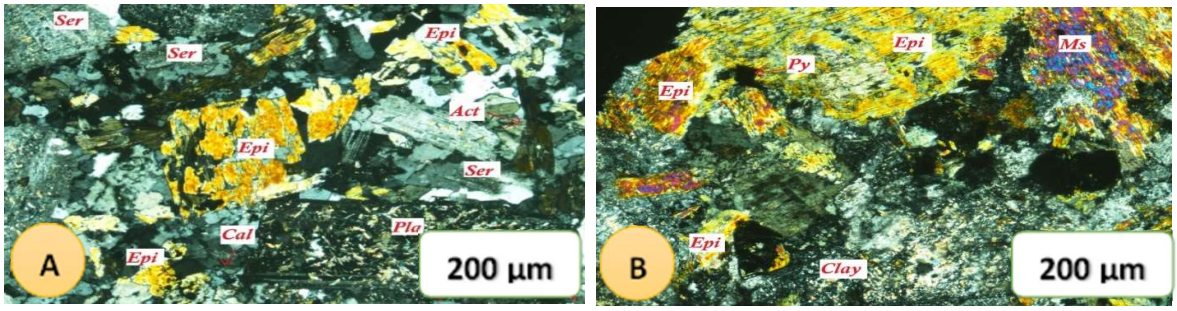

Fig.22. A) Photomicrograph of the Propylitic showing epidote, chlorite, calcite, clay minerals, actinolite and pyrite in altered granodiorite rocks (C.N). B) Photomicrograph showing epidote, muscovite, calcite, clay minerals and pyrite in altered dacite rocks (C.N). (Epi=epidote, Chl =chlorite, Act=actinolite, Mus= Muscovite, Cal= Calcite, clay = clay minerals, Ser= sericite and Pla=plagioclase, Py= Pyrite).

.

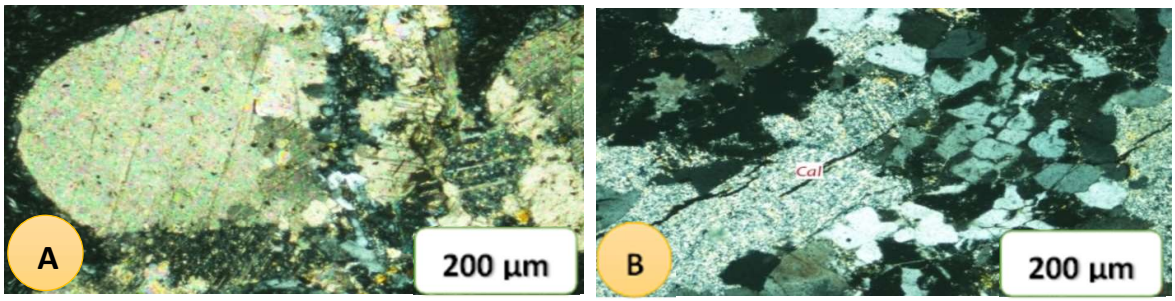

Fig.23. A) Photomicrograph of the carbonatization showing calcite that has filled an amygdule in a highly altered dacite rocks (C.N). B) Photomicrograph of the carbonatization showing orthoclase is highly altered to calcite, biotite is highly altered to muscovite in a highly altered alkali granite rock. (Cal= Calcite, Bt = Bioti, Ser= sericite).

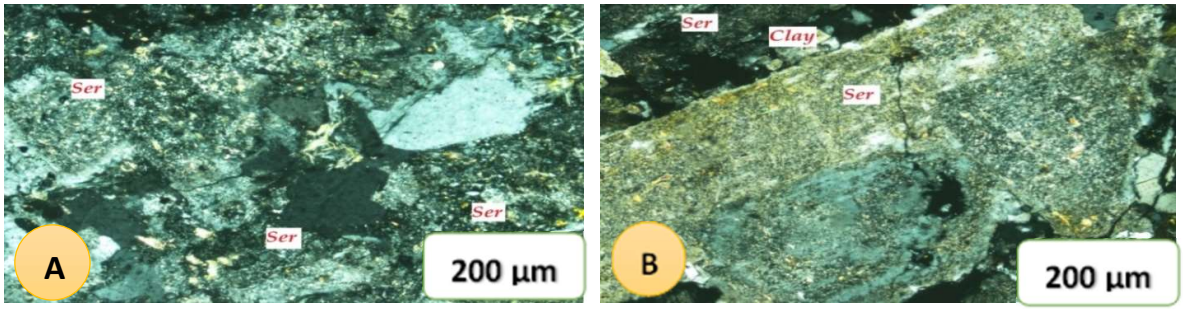

Fig.24. A) Photomicrograph showing sericite is spread widely with opaque minerals in the dacite rocks (C.N). B) Photomicrograph showing phenocrysts of altered plagioclase to sericite and clay minerals in the alkali granite rocks (C.N).

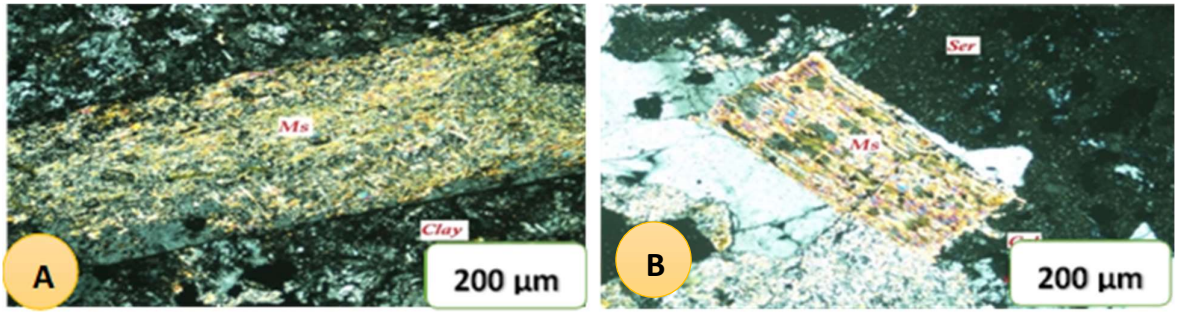

Fig. .25 A) Photomicrograph of the muscovite alteration showing large plagioclase feldspar crystal altered to muscovite in the dacite rocks (C.N). B) Photomicrograph showing feldspar crystal altered to muscovite in the altered syenogranite rocks. (Ms= Muscovite, clay = clay minerals, Ser= sericite).

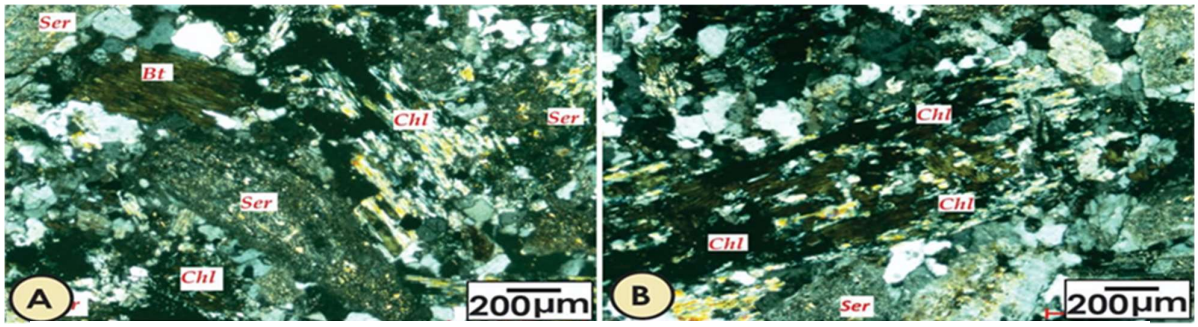

Fig.26 A) Photomicrograph of chloritization alteration showing biotite, chlorite, epidote and sericite (C.N). B) Photomicrograph of chloritization alteration showing flakes of altered biotite to chlorite, associating with altered plagioclase. (C.N.). (Ser=sericite, Chl=chlorite, clay= clay minerals, Bt= Biotite, and Pla=plagioclase

2. Ore mineralogy of auriferous quartz veins

Some selected samples from the quartz veins were examined by a reflected microscope and scanning Electron microscope (SEM/EDX) at the Central Laboratories of the Egyptian Mineral Resources Authority to identify the different ore minerals. The main ore minerals are represented by gold, pyrite, silver, barite, hematite and goethite.

Gold occurs as isolated native disseminated grains in pure state (Fig. 28) and has bright golden yellow colour. Pyrite occurs as fine to medium grained, disseminated subhedral to enhedral crystals (Fig. 29) and is frequently replaced by goethite. Silver occurs as fine discrete grains associated with copper (Fig. 30). Hematite occurs as euhedral to subhedral flake crystals, mostly as a primary mineral (Fig. 31). Barite occurs as euhedral to subhedral crystals with two sets of cleavage (Fig. 32).

3. Paragenetic sequence

The mineral paragenesis of the auriferous quartz veins is based on the data obtained from transmitted and reflected microscope as well as scanning electron microscope. The mutual texture, structural relations and replacement features revealed two main stages of ore mineralization in Makhrag El Ebl gold deposit as shown in (Table 4). The ore mineral stage was started by the formation of oxide minerals (hematite) followed by the formation of primary sulphide minerals (pyrite) and barite at the early stage of hydrothermal phase. Gold and silver native minerals belong to the late stage of hydrothermal Phase. Additionally, pyrite replaced by goethite as a result of metasomatic replacement process. Goethite is the common oxidation products of iron sulphide

4. Quality of the gold ore in the quartz veins and altered rocks

Gold grade refer to the quality of the gold ore. A high quality of gold deposit has gold ore concentration between 8 and 10 g/ton, while a low quality of gold deposit has gold ore concentration between 1 and 4 g/ton.

Eight samples of quartz veins were analyzed for gold content, using the fire assay method. The results showed that gold content in these samples ranges from 0.19 to 12.68 g/t. (Table 5A). Accordingly, the present auriferous quartz veins is retaining to low grad (av. 2.51 g/t).

Eight samples from the different alteration types were analyzed for gold content using fire assay method. The results showed that gold content in these altered samples ranges from 0. 18 to 1.23 g/t (Table 5B). Accordingly, the gold concentration in the altered rocks pertaining to the extremely low grade (ave. 0.53 g/t).

Table 3: Chemical analysis of major oxides (wt. %) and trace elements (ppm) for the altered types in the Wadi Makhrag El Ebl area

Altered type	Ferrugination	Argilization	Carbonatization		Chloritization	Muscovite alteration	Propylitization	silicification	
Sample No	*D2S11a*	*A9C*	*V5*	*A3a*	*D2S3a*	*A26a*	*A1*	*A2a*	*D2S8a*
Major Oxides (%)									
SiO_2	48.30	29.36	56.30	59.12	51.30	55.64	50.11	96.69	95.80
TiO_2	0.21	0.47	0.88	0.50	0.56	0.61	0.53	0.01	0.05
Al_2O_3	3.77	36.10	7.60	9.60	10.80	20.34	13.38	0.43	1.19
FeO	14.30	2.14	3.90	1.80	7.40	1.76	3.10	0.57	0.39
Fe_2O_3	27.50	6.11	6.94	2.20	10.60	2.48	5.50	1.60	1.31
MnO	0.38	0.36	0.32	0.07	0.06	0.09	0.07	0.01	0.01
MgO	2.79	4.11	6.37	5.40	9.12	1.33	0.95	0.02	0.02
CaO	0.58	4.90	10.20	12.64	1.64	0.61	0.82	0.21	0.19
Na_2O	0.38	7.12	2.53	3.80	2.94	3.61	2.95	0.14	0.34
K_2O	<0.01	5.60	1.31	3.87	3.12	12.64	6.80	0.03	0.48
P_2O_5	0.17	0.24	0.20	0.15	0.15	0.15	0.12	0.01	<0.01
LOI	1.97	3.70	3.61	1.17	2.47	1.15	15.85	0.28	0.42
Total	100.35	100.21	100.15	100.32	100.16	100.41	100.18	100.00	100.20
Trace elements (ppm)									
V	75.8	78.7	64	59.1	74.5	60.6	95.5	66.4	61.9
Cr	52.9	73	59.5	59.7	133.5	79.6	73.6	61.2	58.3
Ni	20.5	13.9	22	22.3	50.7	22.4	27.1	24	23.1
Cu	19.6	134	46.2	10.1	1637.1	166.7	446.2	42.8	67
Zn	38.2	14.2	2	51.6	26	14.5	16.1	2	6
Co	16.2	29.1	11.9	11.5	26.4	12.7	17	11.4	13.4
Rb	100.1	114.2	109.4	103.3	90.9	118.2	124.1	108	112
Sr	507	302	321.1	519.4	623.8	270.8	560.4	317.6	309.7
Y	16	18.7	14.8	15.2	15.9	19.1	17.5	13.4	12.4
Zr	229.5	200.1	184.2	200.6	234.4	177.1	236.3	180.2	197
Nb	12.4	12.4	10.7	11.8	12.1	10.3	12.3	11.9	11.3
Ba	1208.3	2914	1997	1046.5	1499.9	1258.3	1.40%	2009	1996
La	51.6	62.7	42.7	27.5	36.3	39.9	44.3	40.1	36.7
Yb	3	1.5	3.3	5.3	10.9	1.9	5.2	3	4.6
Ta	2	2.2	2	1.8	2.9	1.88	2.3	1.7	1.55
Pb	17.1	11.7	9.3	14.6	18.5	19.3	14.9	9	13.8
Th	21.3	12.9	9.1	19.5	23.4	8.6	23.5	11.2	14.7

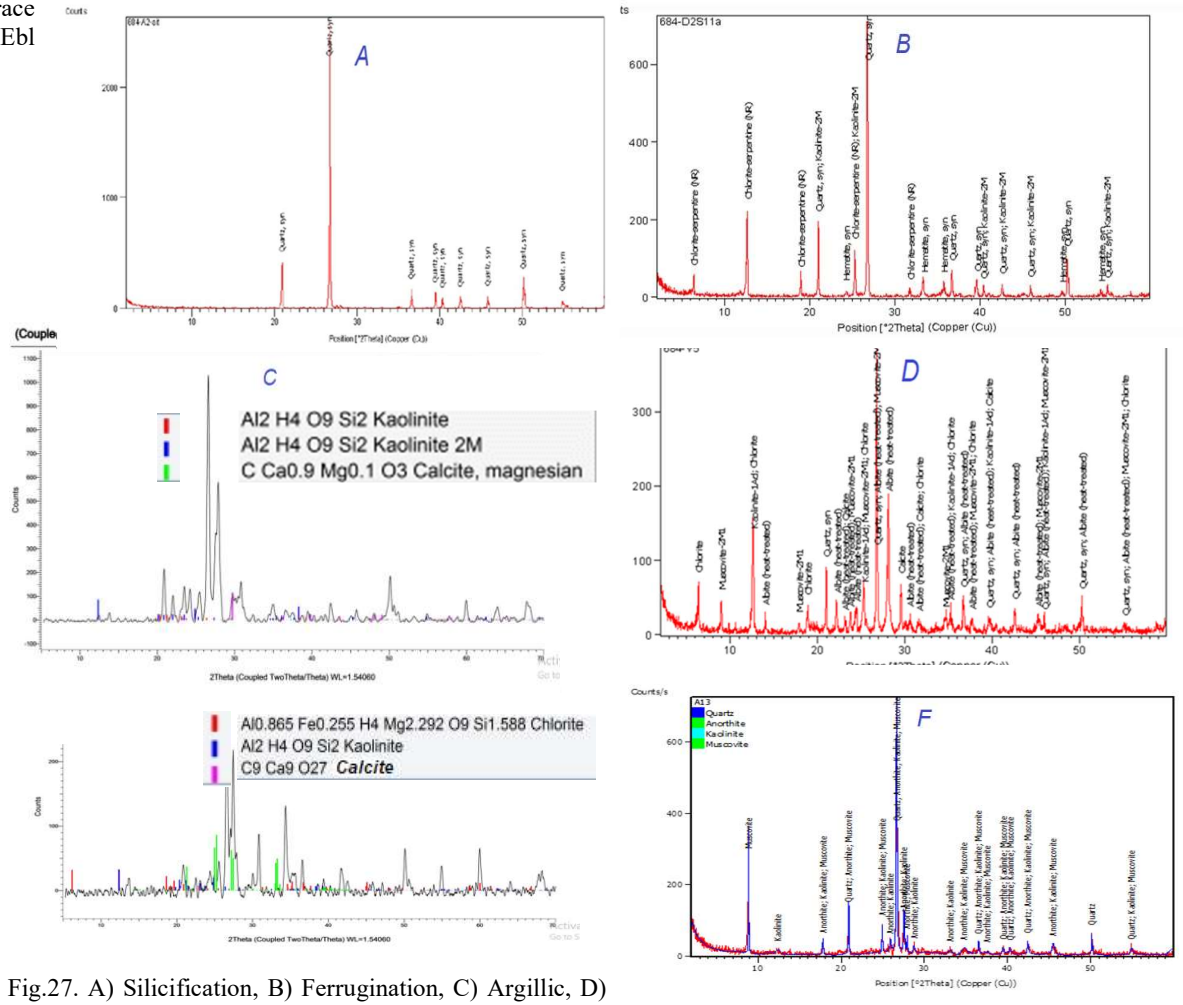

Fig.27. A) Silicification, B) Ferrugination, C) Argillic, D) Propylitic alteration, E) Carbonatization and F) Muscovite alteration.

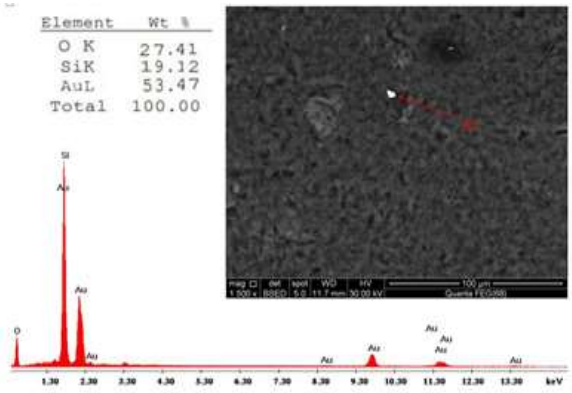

Fig. 28. SEM image and EDX analysis data of gold crystal.

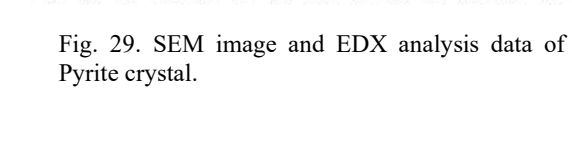

Fig. 29. SEM image and EDX analysis data of Pyrite crystal.

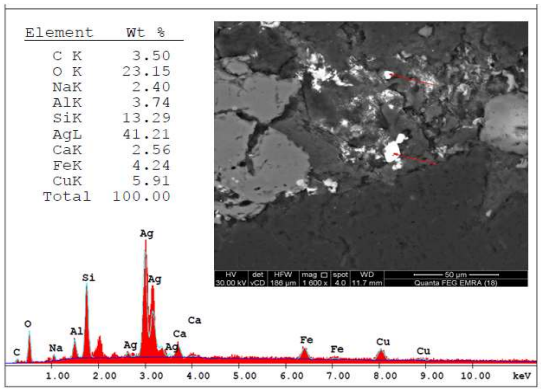

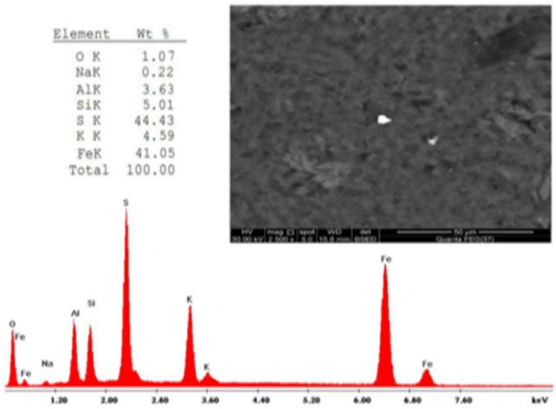

Fig. 30. SEM image and EDX analysis data of Silver

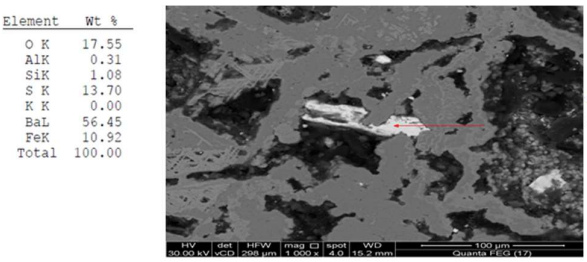

Fig. 31. SEM image and EDX analysis data of hematite.

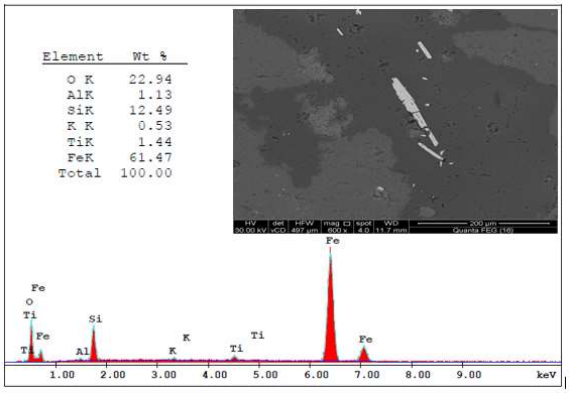

Fig. 32. SEM image and EDX analysis data of barite and hematite crystal

Table 4: paragenetic sequence of the ore minerals at Makhrag El-Ebl.

Ore minerals	Stages of mintralization		
	Hydrothermal		Supergene phase
	Early phase	Late phase	
Hematite	—		
Pyrite	—		
Barite	—		
Gold		—	
Silver		—	
Goethite			—

Table (5A and 5B): Gold fire assay data for the quartz vein samples and alteration samples from Wadi Makhrag El Ebl area.

A Quartz veins	Sample No.	Concentration Au (gm./ton)
	A1	0.19
	A2	1.49
	A3	0.36
	A4	2.42
	A5	2.39
	E1	12.68
	E2	0.31
	A16	0.26
Average = 8 samples	----------	2.51

B Alteration samples	Alteration type	Sample No.	Concentration Au (gm/ton)
	Propylitic	A1	0.34
	Silicification	A2	1.23
	Muscovite alt.	A26	0.57
	Argillic	A13	0.6
		A9	0.49
	Carbonatization	A3	0.18
	Ferrugination	D2S11	0.42
	chloritization	D2S3	0.38
Average = 8 samples		---------	0.53

5. SUMMARY AND CONCLUSION

The present study deals with geology, petrography, geochemistry, alteration zones, and gold bearing quartz veins mineralizations of Wadi Makhrag El Ebl area, North Eastern Desert, Egypt.

Geologically, the study area is covered mainly by Neoproterozoic Pan-African basement rocks. These rocks are classified according to their relative age relations into the following rock unit's granodiorite rocks, Dokhan volcanics, syenogranites, alkali granites, dykes and veins.

Petrographically, granodiorites showing equigranular, hypidiomorphic, perthitic, graphic and piokilitic textures. It is composed mainly of plagioclase, alkali feldspar and quartz associated with minor biotite and hornblende. Dokhan volcanic is unequigranular, displaying several amygdaloidal and porphyritic textures. Dacite is composed mainly of phenocrysts of plagioclase and quartz embedded in groundmass composed of very fine-grained aggregates of plagioclase, quartz, alkali feldspar, and biotite associated with minor amount of muscovite in addition to rare opaque minerals and iron oxides. Amygdales are filled with chlorite, carbonates (mainly calcite), secondary quartz and epidote. Syenogranite is equigranular hypidiomorphic texture. It is composed mainly of quartz, alkali-feldspar, plagioclase and rare biotite. Alkali granites are characterized by equigranular hypidiomorphic texture. It is essentially composed of plagioclase, alkali feldspar, quartz, hornblende and biotite.

Geochemically, granodiorites rocks are of calc-alkaline magma type, formed of compressional environment and emplaced in an island arc tectonic environment. The Dokhan volcanics are mainly of dacites and have calc-alkaline magma type and formed at transitional tectonic setting between island arc and within plate. Younger granites revealed that they are of syenogranite and alkali

granites. They have alkaline magma type and formed in within plate tectonic setting (extensional environments). The studied younger granites were crystalized at depth > 30 km fall in relatively from 1 to 5 k-bar and temperature ranging between 700 and 800ºC indicating that they were probably formed at moderate levels in the crust. Several source rocks have been postulated to explain the generation of granitic magmas by partial melting mechanism. Partial melting under variable conditions of various source rocks produces granitic melts of different composition.Petrographical studies accompanied by XRD and geochemical analysis for the **altered rocks** revealed eight main facies including: Silicification, Ferrugination, Chloritization, Sericitization, Propylitization, Argillization, Muscovite alteration and Carbonatization.

Two main stages of ore mineralization in Makhrag El Ebl gold deposit can be identified. The early stage caused the formation of oxide (Hematite), sulphide (pyrite) minerals and barite. The late stage of hydrothermal phase caused the formation of gold and silver native minerals. This paragenetic sequence mineral originated from the hydrothermal signals that produce the epigenetic ore- filled veins and fissures to the supergene enrichment process that occurred and the surface weathering conditions.

Gold grade in the auriferous quartz veins pertaining to low grade (av. 2.51 g/t.) while the gold grade in the altered rocks pertaining to extremely low grade (av. 0.53 g/t.)

REFERENCES

Botros, N.S. and Wetait, M.A., 1997: Possible porphyry copper mineralization in South Um Monqul, Eastern Desert, Egypt. Egypt. Jour. Geol., V. 41(1), P. 175-196.

Condie, K.C., 1973: Archaean magmatism and crustal thickening. Geol Soc Amer Bull 84: 2981–2992

Cox, K.G.; Bell, J.D. and Pankhurst, R.J., 1979: The Interpretation of Igneous Rocks. London, Allen and Unwin, 450 p.

El-Ramly, M.F., Ivaanov, S.S., Kochin, G.C., 1970: The occurence of gold in the Eastern Desert of Egypt. Studies on some mineral deposits of Egypt. Part I, Sec. A, Metallic Minerals. Geol. Surv. Egypt, 53 – 63Irvine, T.N., Baragar, W.R.A., 1971: A guide to the chemical classification of the common volcanic rocks. Can. Jour. Earth. Sc. 8, 523-548p.

Irvine, T.N., Baragar, W.R.A., 1971: A guide to the chemical classification of the common volcanic rocks. Can. Jour. Earth. Sc. 8, 523-548p.

Le Maitre, R.W. (1984): A proposal by the IUGS subcommisson on the systematic of igneous rocks for a chemical classification of volcanic rocks based on the total alkali silica (TAS) diagram. Aust. J. Earth. Sci., 34, P. 243-255.

Luth WC, Jahns RH, Tuttle OF (1964): The granite system at pressures of 4 to 10 kilobars. J Geophys Res 69: 759–773.

Maniar, P.D. and Piccoli, P.M., 1989: Tectonic discriminations of granitoids. Geol. Soc. Amer. Bull., 6, 129-198.

Myers, R. E., and MacLean, W. H., 1983: The geology of the New Insco copper deposit, Noranda district, Quebec: Canadian Jour. Earth Sci., v. 20, p. 1291-1304.

Pearce, J.A., Gale, G.H., 1977: Identification of ore deposition environment from trace element geochemistry of associated igneous host rocks. In: Volcanic Processes in ore Genesis. Inst. Min. and Metallurgy, Geol. Soc. London, Spec. Publ. 7, 14-24.

Pearce, J.A., Harris, N.B.W. and Tindle, A.G., 1984: Trace element discrimination diagrams for the tectonic interpretation of granitic rocks. Jour. Petrol., 25, 956-983.

Que and Allen, 1996: Sericitization of plagioclase in the Rosses Granite Complex, Co. Donegal, Ireland. Mineralogical Magazine1996 vol. 60 (pg. 927-936).

Streckeisen, A., 1976: Classification of the common igneous rocks by means of their chemical composition. A provisional attempt. N. Jb. Miner. 1-15.

Tuttle, O.F., and Bowen,N.L. (1958): Origin of granite in the light of experimental studies in the system Na Al Si_3O_8-SiO_2- H_2O. Geol. Soc. Amer. Mem., V.74, 153p.

Wilson, J. Q. 1989. Bureaucracy: What Government Agencies Do and Why They Do It. New York: Basic Books

Wright, J.B., 1969: Alkalinity ratio and its application to questions of non-Orogenic granite genesis. Geol. Mag., 106, 307-384.